Electromagnetic Non-Destructive Evaluation (XXIII)
G.Y. Tian and B. Gao (Eds.)

doi:10.3233/SAEM200037

Multi-Channel IoT-Based Ensemble-Features Fault Diagnosis for Machine Condition Monitoring

Shang Gao[1], Cuicui Du
Nanjing University of Science and Technology, the school of mechanical engineer, 210094, Nanjing

Abstract. This paper proposes a multi-channel internet of things (IoT)-based industrial wireless sensor network (IWSN) with ensemble-features fault diagnosis for machine condition monitoring and fault diagnosis. In this paper, the rolling bearing is taken as an example of monitored industrial equipment due to its wide use in industrial processes. The rolling bearing vibration signals are measured for further processing and analysis. On-sensor node ensemble feature extraction and fault diagnosis using Back Propagation network are then investigated to address the tension between the higher system requirements of IWSNs and the resource-constrained characteristics of sensor nodes. A two-step classifier fusion approach using Dempster-Shafer theory is also explored to increase diagnosis result quality. Four rolling bearing operating in cage fracture, rolling ball spalling, inner ring spalling and outer ring spalling are monitored to evaluate the proposed system. The final fault diagnosis results using the proposed classifier fusion approach give a result certainty of at least 94.21%, proving the feasibility of the proposed method to identify the bearing-fault patterns. This paper is conducted to provide new insights into how a high-accuracy IoT-based ensemble-features fault diagnosis algorithm is designed and further giving advisable reference to more IWSNs scenarios.

Keywords. IoT, wireless sensor networks (WSNs), fault diagnosis, BP network, Dempster-Shafer theory

1. Introduction

Machine fault diagnosis is becoming increasingly important to meet the higher demand of safety, reliablity and efficiency in many industrial areas. [1, 2]. As the key components of machinery, the rolling bearings have been widely applied in most industrial sectors, [3]. Due to artificial errors, material defects, and inadequate operations of the bearing, various incipient defects of rolling bearings may occur, and potentially lead to a series of unforeseen damages [4]. Hence, bearing-fault diagnosis is of paramount significance to improve the availability, increase the operating efficiency, and ensure the safe operation of the mechanical system [5].

Generally, bearing fault diagnosis depending on on-line monitoring vibration signal of critical devices includes three stages: signal processing, feature extraction,

[1] Shang Gao, Corresponding author, the school of mechanical engineer, Nanjing University of Science and Technology, E-mail: shang.gao@njust.edu.cn.

and classification recognition [6]. Currently, in many industrial fields, bearing fault diagnosis relies on the wired systems, which features as high reliability, but expensive maintenance cost, time-consuming [7]. Alternately, the wireless sensor networks (WSNs) have many inherent advantages including less weight, distributed operation, ease installation and relatively low-cost manufacturing, which make them as a promising approach for fault diagnosis [8]. As a new technology, the WSN has drawn more attentions in structural health monitoring (SHM) and NDT&E areas and numerous researchers have yielded some achievements [9-11]. Our previous work demonstrated a new multi-channel MEMS-based Low-Power Wide-Area Network (LPWAN) incorporating LoRa with NB-IoT for machine vibration monitoring [12]. Due to the constrained resources including limited computational ability, communication bandwidth and battery energy in WSN monitoring systems, the on-line feature extraction[13] and fault diagnosis is a promising approach to reduce the quantity of transmitted data, save energy and prolong node lifetime.

In WSN, the single sensor cannot capture more useful data for device fault diagnosis. In this case, the quality of IWSNs and the diagnosis uncertainty are impacted in noise and interference environment. However, if different sensors are adopted, the measurement accuracy of data fusion can be enhanced. Data fusion based on multiple sensors can effectively reduce the amount of data information which saves the resources and energy of the measuring data. The data fusion techniques such as the Bayesian method [14] and fuzzy data fusion [15] have been reported. As a new promising data fusion technique, the Dempster–Shafer theory does not require the knowledge of the prior probability and conditional probability relationships of data. This method based on wired sensor systems for fault diagnosis has been applied on induction motor [16], diesel engine cooling system [17], and railway track circuit [18]. The method has been proved as an efficient classifier fusion approach to increase diagnosis result quality[19].

In this paper, the following design strategies have been adopted to explore the applicability of data fusion for fault diagnosis in WSNs.

1) We propose a new IoT-based Ensemble-Features IWSN for machine fault diagnosis. A local-processing distinct ensemble -extraction algorithm in time-domain and frequency-domain is presented, which contributes to the low power consumption, low cost, and covering all the typical characteristics of vibration signals and current signals.

2) We also extends the previous WSN data fusion by applying Dempster–Shafer theory to for industrial condition monitoring and fault diagnosis.

The remainder of this paper is organized as follows. The system architecture and implementation methodology is briefly introduced in Section 2. The experimental evaluation of the proposed system is given in Section 3. Finally, Section 4 presents the overall conclusions.

2. System Architecture and Implementation

The rolling bearing condition fault diagnosis system with two-classifier data fusion is illustrated in Fig. 1. This IWSN consists of multi-channel sink node and multiple sensor nodes. Some sensor nodes measure the vibration on the head of the motor while other sensor nodes acquire the stator current signal. End node can achieve the signal conditioning, data acquisition, feature extraction (vibration and current

signal), while the multi-channel sink node makes data fusion decision and local fault classification. The diagnosis results are displayed on the centralized computer.

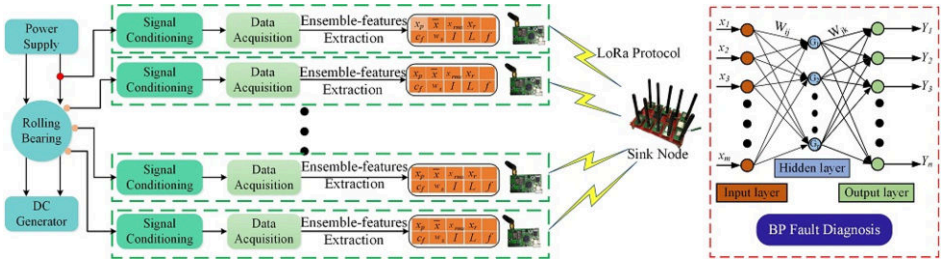

Fig.1 Schematic diagram of the proposed system

2.1. The LoRa-based Multi-Features Extraction Sensor Node (LMESN) and sink node

As is shown in Fig.1, the LMESN is mainly consisted of data acquisition unit, wireless communication unit, wireless unit, power module. The core of data acquisition unit is TI ADS8688AT chip having 16-bit resolution Analog-to-Digital Converter (ADC) and conversion rate of up to 100 kHz. With regard to the data sensing unit, the ADXL345 micro-electromechanical systems (MEMS) accelerometer with 12-bit resolution of measurement ranging from $\pm 2\ g$ to $\pm 16\ g$ and 3.9 mg / LSB sensitivity is integrated into the LMESN. The collected data are sent to the local-processing feature extraction unit for performing the feature extraction of vibration signal. As for the wireless communication, a low-power RF chip Silicon SX1278 based on LoRa protocol, which can offer a theoretical maximum transfer speed of 500 $kbps$. The SX1278 in wireless unit is connected to STM32F407 processor through SPI ports for exchanging commands and transmitting wireless data. Our previous work has proposed a multi-channel sink node integrated multiple LoRa modules and NB-IoT modules for machine vibration monitoring[12].

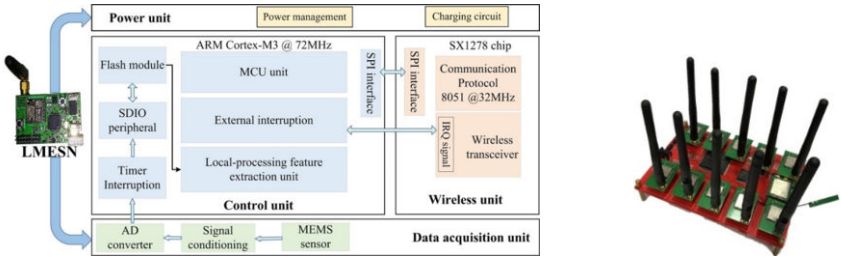

(a) (b)

Figure 2. The architecture of (a)LMESN and (b)multi-channel sink node

2.2. Feature-extraction Design

As shown in Fig.3, the architecture of the rolling bearing is consisted of the rolling ball, cage, inner ring and outer ring. In this respect, D is the bearing pitch, d is the diameter of rolling ball and α is the angle between the forced direction of rolling ball and the inner and outer vertical lines. Four common faults of the rolling bearing are

F1="cage fracture," F2="rolling ball spalling," F3="inner ring spalling," and F4="outer ring spalling" respectively.

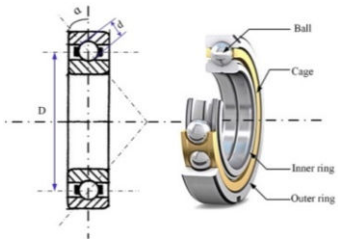

Figure 3. Structure of a rolling bearing

This sensor node extracts the time-domain data features for fault diagnosis from the raw digital data stream. The time-domain characteristic parameters mainly include dimensional parameters (mean value, peak value, root mean square value, square root amplitude) and non-dimensional parameters (tolerance index). Ten frequently occurring frequency components (20480 samples within one fast Fourier transform) were counted and selected as the fault features in the frequency domain. These fault features will be used to classify the healthy rolling bearing. The definition of these parameters is shown in Table 1.

Continuous amplitude monitoring of the stator current signal is used to identify motor load changes and find the abrupt change of load. In addition, periodic load torque changes with the rotational speed can affect the stator current signal spectrum and produce the current harmonics. In this paper, the load changes are tested by the modulation of a resistor connected to a generator used as a load, which is not a cyclic load variation, and do not give other current harmonics. As for the stator current signal, peak-to-peak amplitude and variance value in the time domain are selected as features for fault diagnosis. The selected fault features in this experiment are summarized in Table I.

Table 1. Dimensional and non-dimensional parameters of vibration and current signal

Signal		Time Domain	Frequency Domain
Vibration	Dimensional parameters	Peak value $x_{pv} = max(\lvert x_i \rvert)$ Mean value $\overline{x} = (\sum_{i=1}^{N} \lvert x_i \rvert) / N$ Root mean square value $x_{rms} = \sqrt{(\sum_{i=1}^{N} x_i^2) / N}$ Square root amplitude $x_r = \left\lvert (\sum_{i=1}^{N} \sqrt{\lvert x_i \rvert}) / N \right\rvert^2$	(2,3) f_b, (5,6) f_b, (7,9) f_b, (11,13) f_b, (15,17) f_b, (18,20) f_b, (21,23) f_b, (26,62) f_b, (68,93) f_b, >93 f_b
	Non-dimensional parameters	Kurtosis index $\beta = (\sum_{i=1}^{N} x_i^4) / N$	
Current	Dimensional parameters	Peak value $x_{pc} = max(\lvert x_i \rvert)$	n/a

* $\{x_i\}(i = 1 \sim N)$ is a series of discrete signals (N is data points), the frequency component is about 100Hz, twice of the line frequency. f_b is the resolution of FFT, $f_b = 5Hz$

2.3. Neural Network Classifier

In this paper, a BP neural network is used to achieve local fault classification. It includes several hidden layers and output layers corresponding to five rolling bearing working condition. The log-sigmoid function is selected as the hidden layer and output layer neuron activation function which is defined as:

$$\log sig(n) = \frac{1}{(1+\exp(-n))} \tag{1}$$

The input vibration or current signals of the neural network are 16 fault features including 10 frequency features, and 6 time-domain features ($x_1, x_2, ..., x_{16}$). In the classifier, the output range of the neural network classifier was (0, 1) which indicates the diagnosis probability. The training error of the neural network was set at 0.01which can be embedded in the local classifier on the sensor node for online primary fault diagnosis. The corresponding ideal output {1, 0, 0, 0, 0} of the neural network classifier if the motor is a healthy.

Dempster–Shafer theory assigns a belief mass to each element of the power set. Shown as (2), a basic belief assignment (BBA), called m in the following, is a function mapping from 2Θ to [0, 1], provided that the sum of all basic belief masses is equal to one and the mass of null set is zero:

$$m: 2^{\theta} \to [0,1] \text{ if } \sum_{A \subseteq \Theta} m(A) = 1 \quad \text{and} \quad m(\varnothing) = 0 \,. \tag{2}$$

According to (2), the sum of all basic belief masses is equal to one. Therefore, the outputs of neural network classifier $y(\mathrm{B_i})$ need to be normalized as follows:

$$m(B_i) = \frac{y(B_i)}{\sum_{i=1}^{4} y(B_i)} \tag{3}$$

where B_i, i = 1, 2, 3, 4, denotes the four previously described operating conditions of the rolling bearing. The results of the normalized $m(B_i)$ can be used for further decision level classifier fusion.

2.4. Decision Level Fusion

Data level fusion processes are often categorized as data level fusion, feature level fusion, or decision level fusion. Decision level fusion combines the primary recognition data from each sensor and makes an accurate decision. It utilizes the computing capability of individual low-level sensors and reduces the communication throughput. Therefore, in this paper, decision level fusion by Dempster–Shafer theory was selected to combine the outputs of the local neural network classifiers.

3. Experimental Verification

To evaluate the performance of the proposed bearing fault diagnosis method, a series of experiments are conducted. The experimental setup is shown in Fig.4. Four LMESNs nodes are installed on a Drivetrain Diagnostics Simulator (DDS) for implementing to acquire vibration signal of rolling bearing. Then, the processed

vibration signals are sent to the sink node. Additionally, the sampling frequency of the system is configured to the value of 10.24 kHz, coupling with sampling length set to 20480. The rotating speed of the testing bearing is set to around 1310 r/min.

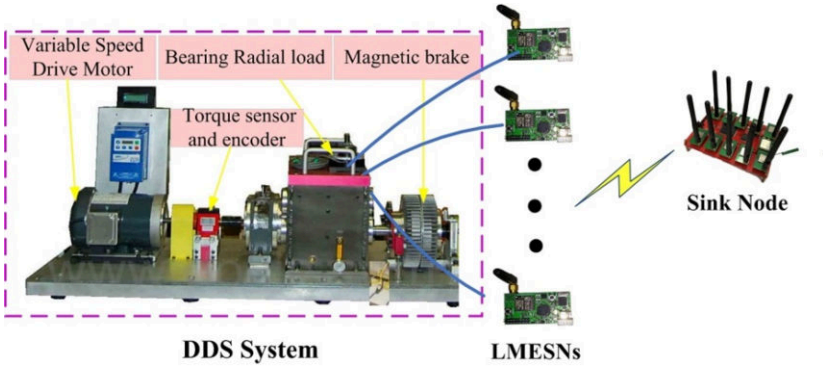

Fig.4 Wireless experimental test for rolling bearings based on DDS system

In this section, to investigate the influence of the number of hidden layer nodes, vibration parameters, current parameter on the fault classification accuracy, we make a detailed comparative analysis under vibration parameters(x_{pv} , $\bar{x}$, x_{rms} , x_r , β),the vibration and current parameters(x_{pv} , $\bar{x}$, x_{rms} , x_r , β and x_{pc}) and the time-frequency-domain parameters (x_{pv} , $\bar{x}$, x_{rms} , x_r , x_{pc} , β and f) respectively, as hidden layer nodes are set to 5, 6, 7, 8, 9, 10. As is shown in Fig. 5 (a), the average classification accuracies under the vibration parameters are below 70%, due to the indistinct differences between 5 vibration parameters for 5 bearing states. In contrast, it is seen from Fig.5 (b) that all average fault classification accuracies under the vibration and current parameters are above 75%. Due to the vibration parameter and current parameter are two types of parameters, so the fault classification accuracy indicates that the combination of vibration features and current parameter could better reflect the actual information of bearings.

As is shown in Fig.5(c), it is noted that the average fault classification accuracies under the combination of the vibration or current time-domain parameters and vibration frequency-domain parameter are nearly close to 95%, proving that this combination for fault classification accuracy outperforms the time-domain parameters or frequency-domain parameters. Additionally, we can see from the three figures that the classification accuracy can reach the highest level as the number of hidden layer nodes reaches 7. It's also worth mentioning from Fig.5 (c) that the classification accuracies of five bearing state degree recognition are achieved with 95.48% (Normal), 97.84% (F_1), 96.28% (F_2), 96.12% (F_3) and 94.21% (F_4), respectively. Nevertheless, it cannot continuously guarantee a high and stable accuracy rate when the number of hidden layer nodes exceeds 7. The reason is the few hidden layer nodes (P.5 and P.6) contributes to inadequate training, while the excessive hidden layer nodes (P.8, P.9 and P.10) result in too long learning time, larger training error and worse generalization ability. In conclusion, the hidden layer node P.7 is the optimal node for the proposed BPNN, which can reach the highest classification accuracies.

In short, the above comparison analysis results have proved that the selected 6 time-domain parameters and 10 frequency-domain parameters with representative ability of extracted features can provide a more reliable and stable fault classification

accuracy for bearings. In addition, the fault classification accuracies can attain the best performance as the hidden layer node of BPNN is 7.

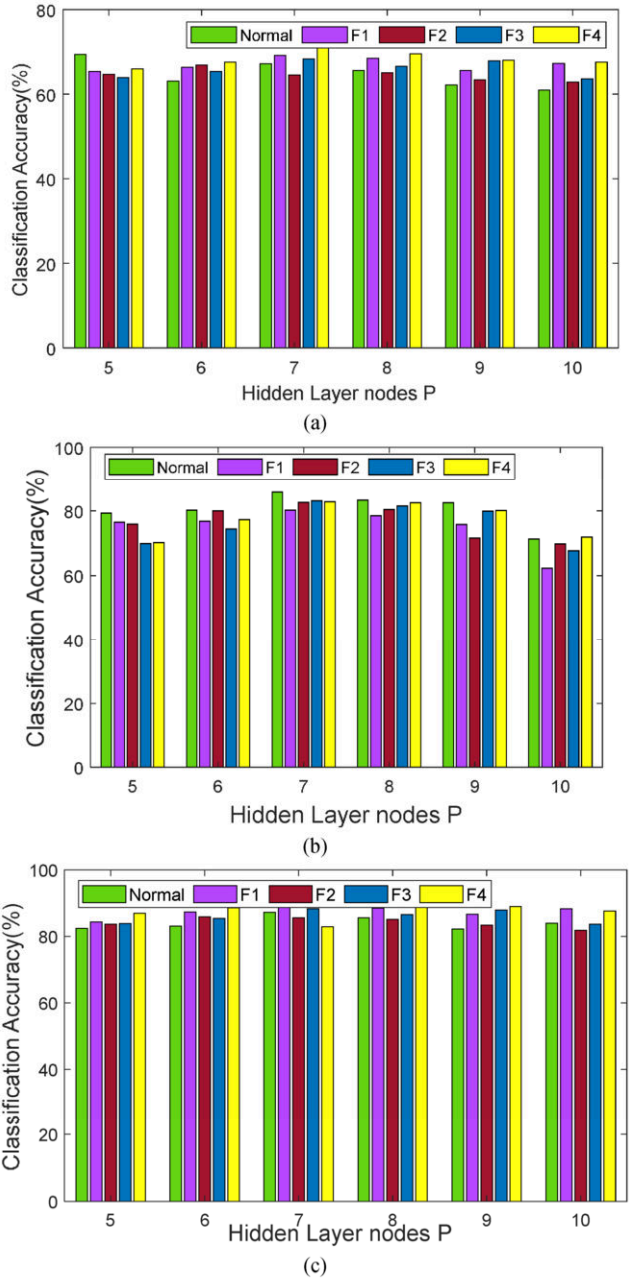

Fig.5. Average fault classification accuracies with different hidden layer nodes of BPNN under different parameters (a) under vibration parameters(x_{pv} , $\bar{x}$, x_{rms} , x_r , β); (b) under the vibration and current parameters (x_{pv} , $\bar{x}$, x_{rms} , x_r , β and x_{pc}); (c) under the time-frequency-domain parameters(x_{pv} , $\bar{x}$, x_{rms} , x_r , x_{pc} , β and f);

4. Conclusion and Discussion

In this paper, we proposed a local-processing ensemble-features fault diagnosis algorithm based on the BP neural network (BPNN) and Dempster–Shafer theory for machine condition monitoring is proposed in this paper. We actualize the LMESN for acquiring vibration and current signals of bearings. In addition, time-domain and frequency-domain vibration signals and time-domain parameters of current signals are extracted as the input vector of the designed BPNN. The feasibility and performance of the proposed method has been verified by a set of comparison experiments on a bearing. Furthermore, considering the key importance of the hidden layer nodes and different number of characteristics to the fault classification accuracy, we conduct many experiments with different hidden layer nodes under different number of characteristics and prove that the average classification accuracies of five bearing state degree recognition under vibration and current parameters reach the highest level as the hidden layer nodes of BPNN P is 7. The proposed strategy is expected to apply in SHM, NDT&E or other multi-sensor monitoring scenarios.

References

[1] R. N. Bell, D. W. McWilliams, P. O'Donnell, C. Singh, and S. J. Wells, "Report of large motor reliability survey of industrial and commercial installation, part I and part II," *IEEE Trans. Ind. Appl.*, vol. 21, no. 4, pp. 853–872, Jul. 1985.

[2] Z. Y. Jiang, Z. W. Li, N. Q. Wu, and M. C. Zhou, "A Petri Net Approach to Fault Diagnosis and Restoration for Power Transmission Systems to Avoid the Output Interruption of Substations," *IEEE Syst J.,* vol. 12, no. 3, pp. 2566-2576, 2018.

[3] Z. Gao, C. Cecati, and S. X. Ding, ''A survey of fault diagnosis and fault-tolerant techniques—Part I: Fault diagnosis with model-based and signal-based approaches,'' *IEEE Trans. Ind. Electron.*, vol. 62, no. 3, pp. 3757–3767, Jun. 2015.

[4] Z. Gao, C. Cecati, and S. X. Ding, ''A survey of fault diagnosis and fault-tolerant techniques—Part II: Fault diagnosis with knowledge-based and hybrid/active approaches,'' *IEEE Trans. Ind. Electron.*, vol. 62, no. 6, pp. 3768–3774, Jun. 2015

[5] Z. W. Wang, Q. H. Zhang, and J. B. Xiong, "Fault Diagnosis of a Rolling Bearing Using Wavelet Packet Denoising and Random Forests," *IEEE Sensors J.*, vol. 17, no. 17, pp.5581-5588, September, 2017.

[6] X. Xue and J. Zhou, ''A hybrid fault diagnosis approach based on mixed-domain state features for rotating machinery,'' *ISA Trans.*, vol. 66, pp. 284–295, Jan. 2017.

[7] A. J. Torabi, M. J. Er, X. Li, B. S. Lim, and G. O. Peen, "Application of Clustering Methods for Online Tool Condition Monitoring and Fault Diagnosis in High-Speed Milling Processes," *IEEE Syst J.,* vol. 10, no. 2, pp. 721-732, 2016.

[8] Y. S. Zhang, Q.W. Gao, Y.X. Lu, D. Sun, Y. Xia, and X. M. Peng, "A Novel Intelligent Method for Bearing Fault Diagnosis Based on Hermitian Scale-Energy Spectrum,"*IEEE Sensors J.,* vol.18, no.16, pp. 6743-6755, 2018.

[9] Y. Y. Peng, W. Qiao, L. Y. Qu, and J. Wang, "Sensor Fault Detection and Isolation for a Wireless Sensor Network-Based Remote Wind Turbine Condition Monitoring System," *IEEE TRANSACTIONS ON INDUSTRY APPLICATIONS*, vol. 54, no. 2, pp. 1072-1079, 2018.

[10] L. Hou, N. W. Bergmann, "Novel Industrial Wireless Sensor Networks for Machine Condition Monitoring and Fault Diagnosis," *IEEE Transactions on Instrumentation and Measurement*, vol. 61, no. 10, pp. 2787-2798, 2012.

[11] Lee H C , Chang Y C , Huang Y S, "A Reliable Wireless Sensor System for Monitoring Mechanical Wear-Out of Parts," *IEEE Transactions on Instrumentation and Measurement*, vol. 63, no.10, pp.2488-2497, 2014

[12] S. Gao, X. H. Zhang, C. C. Du, and Q. Ji, "A Multi-Channel Low-Power Wide-Area Network with High-Accuracy Synchronization Ability for Machine Vibration Monitoring," *IEEE INTERNET OF THINGS*, 2019 (Early Access) Available Online: DOI: 10.1109/JIOT.2019.2895158

[13] R. D. Jesus, and R. Troncoso, "Multirate Signal Processing to Improve FFT-Based Analysis for Detecting Faults in Induction Motors," *IEEE Transactions on Industrial Informatics*, vol.13, no. 3, pp. 1291-1300, 2017.

[14] Kia, S.H., Henao, H., Capolino, G.A.: 'Diagnosis of broken-bar fault in induction machines using discrete wavelet transform without slip estimation', *IEEE Trans. Ind. Appl.*, vol. 45, no. 4, pp. 1395-1404, 2009.

[15] S. Mohanty, K. Gupta, K. S. Raju, "Adaptive fault identification of bearing using empirical mode decomposition–principal component analysis-based average kurtosis technique," IET Science, Measurement & Technology, vol. 11, no. 1, pp. 30-40, 2017.

[16] Sandeep S. Udmale, and Sanjay Kumar Singh, "Application of Spectral Kurtosis and Improved Extreme Learning Machine for Bearing Fault Classification", *IEEE TRANSACTIONS ON INSTRUMENTATION AND MEASUREMENT*., pp. 1-12, 2019. (Early Access)

[17] Q. Fu, B. Jing, P. He, S. Si, and Y. Wang, "Fault feature selection and diagnosis of rolling bearings based on eemd and optimized Elman_AdaBoost algorithm," *IEEE Sensors J.*, vol. 18, no. 12, pp. 5024–5034, Jun. 2018.

[18] He, D., Li, R., Zhu, J., Zada, M.: 'Data mining based full ceramic bearing fault diagnostic system using AE sensors', *IEEE Trans. Neural Netw.*, vol. 22, no. 12, pp. 2202-2031, 2011.

[19] Hou L, Bergmann N W. Novel Industrial Wireless Sensor Networks for Machine Condition Monitoring and Fault Diagnosis[J]. IEEE Transactions on Instrumentation & Measurement, vol. 10, no. 61, pp.2787-2798, 2012.